

Achieving fully-compensated ferrimagnetism through two-dimensional heterojunctions

San-Dong Guo^{1†,*}, Junjie He^{2,†} and Yee Sin Ang³

¹*School of Electronic Engineering, Xi'an University of Posts and Telecommunications, Xi'an 710121, China*

²*KFMCH, Faculty of Science, Charles University, Prague 12843, Czech Republic and*

³*Science, Mathematics and Technology (SMT), Singapore University of Technology and Design (SUTD), 8 Somapah Road, Singapore 487372, Singapore*

In addition to altermagnets, fully-compensated ferrimagnets are another category of collinear magnetic materials that possess zero-net total magnetic moment and exhibit spin-splitting, making them promising for low-energy spintronics, high-density data storage and high-sensitivity sensors. Although many methods, such as alloying, external electric field, Janus engineering, ferroelectric field and spin ordering, have been proposed to achieve fully-compensated ferrimagnetism, these approaches either face experimental difficulties or produce a small spin-splitting or are volatile. Here, we propose to form vertical heterostructures by stacking two different but equally magnetized two-dimensional ferromagnetic materials. If an A-type antiferromagnetic ordering is satisfied, a fully compensated ferrimagnet can be formed. This vertical heterostructure approach is insensitive to lattice matching and stacking manner, thus being more conducive to experimental realization. Through first-principles calculations, we verify our proposal with several examples, focusing in particular on CrI₃/CrGeTe₃ heterojunction composed of experimentally synthesized CrI₃ and CrGeTe₃ monolayers. The calculations show that CrI₃/CrGeTe₃ is a fully-compensated ferrimagnet, with pronounced spin-splitting, and that tensile strain is more favorable for achieving fully-compensated ferrimagnetism. Our work provides an experimentally feasible strategy for realizing fully-compensated ferrimagnetism, thereby further advancing the development of this field.

Introduction.— Zero-net-magnetization systems are emerging, which offer superior spintronic performance with ultrahigh data densities, immunity to external perturbations, and femtosecond-scale writing speeds[1, 2]. Although conventional antiferromagnets possess zero net magnetization, the absence of spin-splitting severely limits their practical applications. Recently, altermagnets have garnered significant attentions in the field of magnetism, because they not only possess the zero-net-magnetization of antiferromagnets in real space, but also inherit the spin-splitting characteristics of ferromagnets in momentum space[3–11]. Altermagnets provide an ideal platform for both fundamental science and the practical applications of next-generation information technologies.

In addition to altermagnets, fully-compensated ferrimagnets constitute another category of collinear magnetic materials, characterized by a zero-net magnetic moment and the presence of spin-splitting[12–21]. The two spin sublattices of conventional antiferromagnets or altermagnets are connected by either space inversion/translation (P/τ) or rotational/mirror (C/M) symmetry, but the two spin sublattices in fully-compensated ferrimagnets are not connected by any symmetry. Fully-compensated ferrimagnets, like altermagnets, can also exhibit a range of phenomena, including the anomalous Hall and Nernst effects, non-relativistic spin-polarized currents, and the magneto-optical Kerr effect[20].

Fully-compensated ferrimagnets can be realized through alloying (see Figure 1 (a)), mainly focusing on bulk materials[12–14]. For example, two magnetic atoms with opposite spin polarizations are from 4d and 3d elements from the same chemical group, respectively. If a two-dimensional (2D) system has spin-layer coupling

(A-type antiferromagnetic (AFM) ordering), an electric field can induce fully-compensated ferrimagnetism (see Figure 1 (b)), which can be an external electric field, the built-in field from a Janus structure, or the internal field of ferroelectric polarization[20–27]. Very recently, fully-compensated ferrimagnetism has been experimentally achieved in bilayer CrPS₄ by a perpendicular external electric field[28]. Fully-compensated ferrimagnetism can also be realized by engineering the spin ordering rather than modifying the lattice structure (see Figure 1 (c))[29]. Although many strategies for achieving fully-compensated ferrimagnetism have been proposed, some face experimental challenges (such as that induced by Janus engineering[20–23]), some induce relatively small spin-splitting (such as that induced by sliding ferroelectrics[25–27]), and some are volatile (such as that induced by external electric field[20–24]). Here, we propose to achieve fully compensated ferrimagnetism by stacking two different ferromagnetic (FM) monolayers with the same total magnetic moment to form a heterojunction. Our proposal not only can produce a large non-volatile spin-splitting but also may be relatively easy to implement experimentally.

Approach.— In a fully-compensated ferrimagnet, the two sublattices with opposite spin polarizations are not connected by any symmetry[20]. That is to say, the surrounding environments of the two magnetic atoms with opposite spin polarizations are different. In fact, the magnetic moment of a magnetic atom can be replaced by the total magnetic moment of a primitive cell. If we periodically arrange two primitive cells made of different materials but with the same total magnetic moment, and require that the total magnetic moments of these two

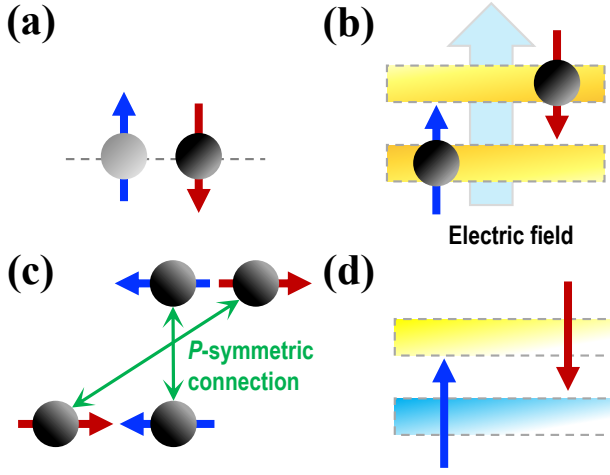


FIG. 1. (Color online) (a): the isovalent alloying can induce fully-compensated ferrimagnetism in PT -antiferromagnets or altermagnets. The black and gray spheres represent, for example, $4d$ and $3d$ elements from the same chemical group, respectively. (b): an electric field can induce fully-compensated ferrimagnetism in PT -antiferromagnets or altermagnets with the layer-dependent opposite spin polarization, which can be an external electric field, the built-in field from a Janus structure, or the internal field of ferroelectric polarization. (c): the spin ordering-induced fully-compensated ferrimagnetism with the system possessing lattice P symmetry. (d): by stacking two different monolayers with the same total magnetic moments together to form the so-called heterojunction, the fully-compensated ferrimagnetism can be induced. In (a), (b), (c), and (d), blue arrows represent spin up, while red arrows represent spin down. In (b), the big arrow represents the electric field. In (c), the green arrows represent the P -symmetric connection between two magnetic atoms.

primitive cells are opposite, then the condition for forming a fully-compensated ferrimagnet as mentioned earlier can be satisfied. The materials involved should preferably be FM, as this is more conducive to the formation of a fully-compensated ferrimagnet with a large global spin-splitting. Of course, the materials involved can also be conventional antiferromagnets and altermagnets, but this may not be favorable for large global spin-splitting.

The 2D materials should be the optimal candidate materials, and periodic arrangement in the form of heterostructure is also the simplest or most experimentally feasible method. As shown in Figure 1 (d), stacking two different monolayers with the same total magnetic moment in an A-type AFM arrangement, which is also known as a heterostructure approach, typically breaks the $[C_2||O]$ (The C_2 is the two-fold rotation perpendicular to the spin axis in spin space, and O means $P/C/M$ in lattice space) symmetry and achieves a fully-compensated ferrimagnet. If the two monolayers are altermagnets, such stacking may result in the bilayer still being an altermagnet. To experimentally verify our proposal, we conduct a detailed discussion on $\text{CrI}_3/\text{CrGeTe}_3$

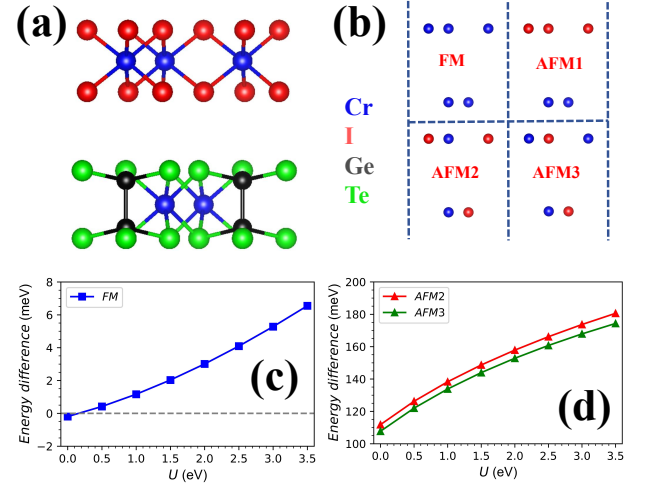


FIG. 2. (Color online) For AB-stacked $\text{CrI}_3/\text{CrGeTe}_3$ heterojunction, (a): the lattice structure; (b): four different magnetic configurations: FM, AFM1, AFM2 and AFM3; (c): the energy of the FM configuration as a function of U with the AFM1 configuration as the reference; (d): the energies of the AFM2 and AFM3 configurations as a function of U with the AFM1 configuration as the reference. In (a), the blue, red, black, and green spheres represent Cr, I, Ge, and Te atoms, respectively. In (b), the blue and red small spheres represent Cr atoms with spin up and spin down, respectively.

heterostructure using experimentally synthesized monolayer CrI_3 and CrGeTe_3 [30, 31] as building blocks, and finally provide a brief illustration with some other examples.

Computational detail.— We perform the spin-polarized first-principles calculations within density functional theory (DFT)[32] and the projector augmented-wave (PAW) method by using the Vienna Ab Initio Simulation Package (VASP)[33–35]. The Perdew-Burke-Ernzerhof generalized gradient approximation (GGA)[36] is used as the exchange-correlation functional. We add Hubbard correction U for d -orbitals of both Cr and Y atoms within the rotationally invariant approach proposed by Dudarev et al[37]. The dispersion-corrected DFT-D3 method[38] is adopted to describe the van der Waals (vdW) interactions. The calculations are carried out with the kinetic energy cutoff of 500 eV, total energy convergence criterion of 10^{-8} eV, and force convergence criterion of $0.01 \text{ eV}\text{\AA}^{-1}$. A vacuum layer exceeding 20 Å along the z -direction is employed to eliminate spurious interactions between periodic images. The Brillouin zone (BZ) is sampled with a $12 \times 12 \times 1$ ($21 \times 21 \times 1$) Monkhorst-Pack k -point meshes for both structural relaxation and electronic structure calculations of $\text{CrI}_3/\text{CrGeTe}_3$ ($\text{YBr}_2/\text{YCl}_2$) heterojunction.

Material realization.— Monolayer CrI_3 has been synthesized experimentally[30], which is composed of three monatomic planes in the sequence I-Cr-I and crystallizes in the $P\bar{3}1m$ space group (No.162). The FM state

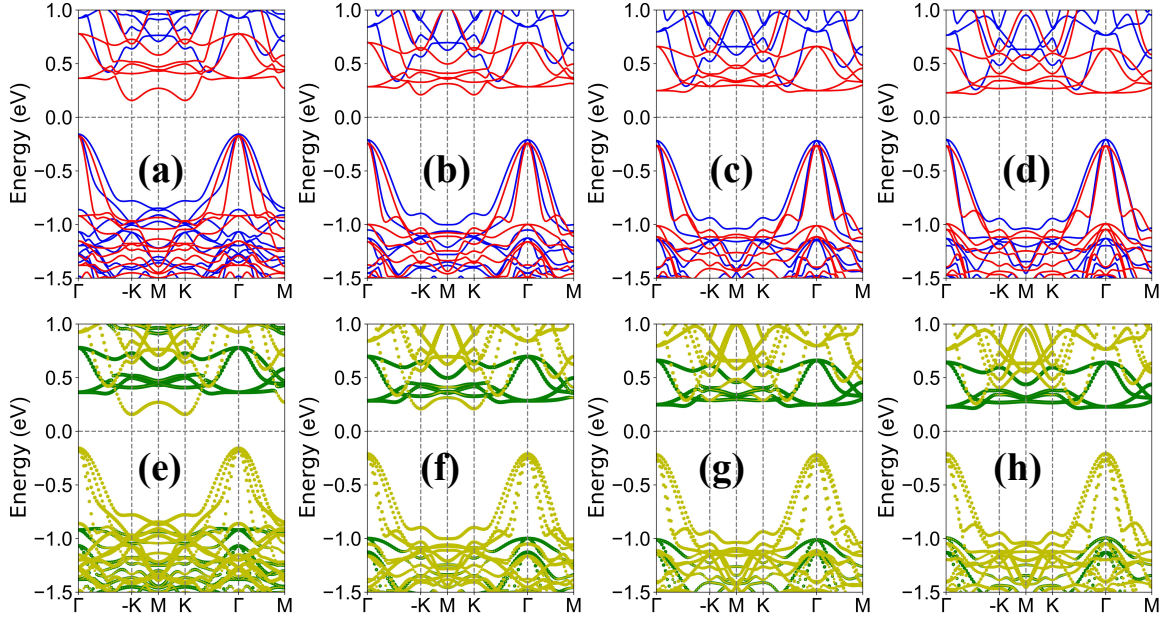


FIG. 3. (Color online) For AB-stacked $\text{CrI}_3/\text{CrGeTe}_3$ heterojunction, the spin-polarized band structures (a, b, c, d) and the layer-projected band structures (e, f, g, h) at $U = 0.00$ (a, e), 1.00 (b, f), 2.00 (c, g), 3.00 (d, h) eV. In (a, b, c, d), the spin-up and spin-down channels are depicted in blue and red. In (e, f, g, h), the yellow and green represent CrGeTe_3 - and CrI_3 -layer characters.

of CrI_3 is the most stable magnetic configuration with total magnetic moments of $6 \mu_B$ per unit cell, and the optimized equilibrium lattice constants are $a=b=7.00 \text{ \AA}$ within GGA. Monolayer CrGeTe_3 can be obtained by replacing I in CrI_3 with Te and additionally adding two Ge atoms at the center of the voids. Each of the two Ge atoms in the unit cell is only threefold coordinated to the Te atoms. These modifications result in CrGeTe_3 and CrI_3 having the same crystallographic space group. The CrGeTe_3 possesses also the FM ground state[31] with total magnetic moments of $6 \mu_B$, and the optimized equilibrium lattice constants are $a=b=6.91 \text{ \AA}$ within GGA. These two monolayers are very suitable for forming heterojunction to validate our proposal.

We stack CrI_3 and CrGeTe_3 to form heterostructures, considering both AA (FIG.S1[39]) and AB (Figure 2 (a)) stacking configurations. They crystallize in the $P31m$ (No.157) and $P3$ (No.143) space group, respectively. The optimized equilibrium lattice constants are $a=b=6.87 \text{ \AA}$ within GGA for both AA and AB stacking configurations. To determine the magnetic ground state, we have examined four magnetic configurations, namely FM, AFM1, AFM2, and AFM3, which are shown in Figure 2 (b). Because the energies of AFM2 and AFM3 are much higher than those of FM and AFM1, we only present here the energy comparisons of FM and AFM1 for AA and AB stacking. The calculations reveal that the AB stacking possesses lower energy, and the AFM1 configuration is the one required as previously proposed. Therefore, taking the AFM1 configuration of the AB stacking as the

reference, the energies of the FM and AFM1 configurations for AA stacking, and the energy of the FM configuration for AB stacking are 26.39, 21.93, and -0.28 meV, respectively. These results show that the FM ordering of the AB stacking has the lowest energy. Because the energy of AA stacking is significantly higher than that of AB stacking, we focus on the AB stacking case in the following discussions.

Nevertheless, electron correlation has a significant impact on the magnetic configuration, electronic structure, and topological properties of 2D magnetic materials[40]. Therefore, we investigate the influence of electron correlation U on the electronic properties of AB-stacked $\text{CrI}_3/\text{CrGeTe}_3$ heterojunction. With AFM1 as the reference, the energies of FM, AFM2, and AFM3 as functions of U are plotted in Figure 2 (c) and (d). Within the range of U considered, the energies of AFM2 and AFM3 are much higher than those of FM and AFM1. When U is just greater than 0.2 eV, AFM1 will become the ground state, which is precisely the magnetic configuration we proposed earlier to achieve fully-compensated ferrimagnetism. It is also clearly seen that increasing the strength of electron correlation is conducive to stabilizing the AFM1 ordering. When AFM1 ordering, the energy band structures with spin- and layer-characteristic projection at representative $U=0.00, 1.00, 2.00$ and 3.00 eV are plotted in Figure 3 (For comparison, the band structure for the case of $U=0.00$ eV is also plotted with the AFM1 ordering.).

Within the range of U considered, all the total

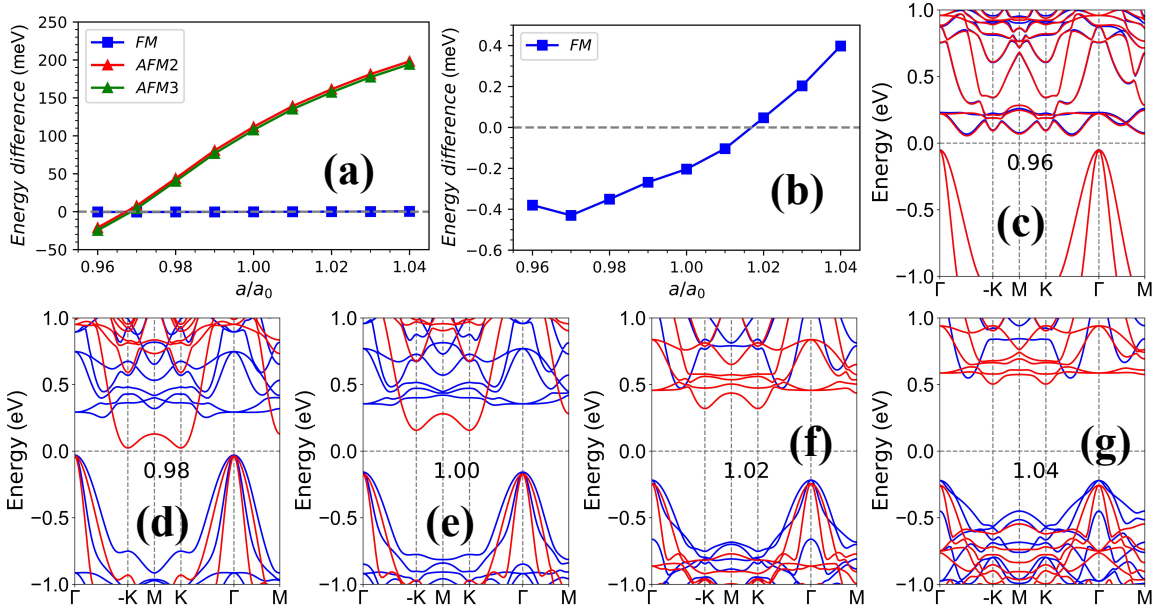


FIG. 4. (Color online) For AB-stacked $\text{CrI}_3/\text{CrGeTe}_3$ heterojunction by GGA ($U=0.00$ eV), (a): the energies of the FM, AFM2, AFM3 configurations as a function of a/a_0 with the AFM1 configuration as the reference; (b): the energy of the FM configuration as a function of a/a_0 with the AFM1 configuration as the reference. (c, d, e, f, g): the spin-polarized band structures at $a/a_0=0.96, 0.98, 1.00, 1.02$ and 1.04 with AFM3, FM, FM, AFM1 and AFM1 orderings, and the spin-up and spin-down channels are depicted in blue and red.

magnetic moments of $\text{CrI}_3/\text{CrGeTe}_3$ heterojunction are strictly $0.00 \mu_B$, which can be guaranteed by the existing band gap[20]. The total magnetic moment can also be calculated by subtracting the number of occupied electrons with spin down from the number of occupied electrons with spin up, which can be confirmed by the integrated densities of states (IDOSs). For the two spin channels of fully-compensated ferrimagnets, IDOSs are not the same across the entire energy range, but it must be the same within the band gap[20]. According to FIG.S2[39], at the representative value of $U=1.00$ eV, the values of IDOSs for the two spin channels are indeed the same within the band gap, further ensuring a zero-net total magnetic moment. For fully-compensated ferrimagnets, the absolute values of the magnetic moments of the magnetic atoms are not strictly equal, which distinguishes them from PT -antiferromagnets and altermagnets[21]. For example $U=1.00$ eV, the absolute values of the magnetic moments of the two Cr atoms in CrGeTe_3 layer are both approximately $3.16 \mu_B$, while those of the two Cr atoms in CrI_3 layer are both approximately $3.10 \mu_B$. This is because the two types of Cr atoms are not symmetrically connected.

In all cases of U , there is a pronounced global spin-splitting in $\text{CrI}_3/\text{CrGeTe}_3$ heterojunction. For altermagnets, there is no spin-splitting at the Γ point, while fully-compensated ferrimagnets can exhibit spin splitting[3, 20]. According to Figure 3, there is a pronounced spin-splitting at the Γ point, which is consistent with the requirements of a fully-compensated ferri-

magnet. The zero-net total magnetic moment and spin-splitting ensure that $\text{CrI}_3/\text{CrGeTe}_3$ heterojunction is indeed a fully-compensated ferrimagnet when U is greater than 0.2 eV. When U is relatively small, the conduction band and valence band of CrGeTe_3 both lie within the band gap of CrI_3 , forming Type-I heterojunction (see Figure 3 (e, f)). When U increases, both the valence and conduction bands of CrGeTe_3 are positioned above the valence and conduction bands of CrI_3 , resulting in a Type-II heterojunction (see Figure 3 (g, h)).

Even when U is less than 0.2 eV in $\text{CrI}_3/\text{CrGeTe}_3$ heterojunction, the fully-compensated ferrimagnetism can be achieved through strain engineering. We use a/a_0 (The a_0 and a represent the lattice parameters without strain and with applied strain, respectively.) to simulate strain, where $a/a_0 < 1$ represents compressive strain, and $a/a_0 > 1$ represents tensile strain. With AFM1 as the reference, the energies of FM, AFM2, and AFM3 as functions of a/a_0 are shown in Figure 4 by GGA ($U=0.00$ eV). Within the range of strain considered, when a/a_0 is less than 0.968 , AFM3 is the ground state; when a/a_0 is greater than 0.968 but less than 1.016 , FM has the lowest energy; and when a/a_0 is greater than 1.016 , AFM1 is in the ground state. When the magnetic ordering of the ground state, the energy band structures with spin-characteristic projection at representative $a/a_0=0.96, 0.98, 1.00, 1.02$ and 1.04 are plotted in Figure 4.

When a/a_0 is greater than 1.106 , $\text{CrI}_3/\text{CrGeTe}_3$ heterojunction exhibits a pronounced spin-splitting, and its

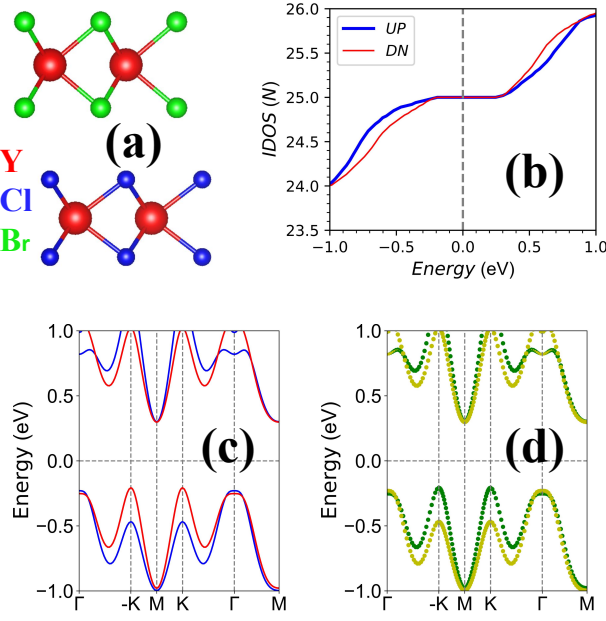


FIG. 5. (Color online) For AB-stacked YBr₂/YCl₂ heterojunction, (a): the crystal structures; (b): the integrated densities of states; (c): the spin-polarized band structures; (d): the layer-projected band structures. In (c), the spin-up and spin-down channels are depicted in blue and red. In (d), the yellow and green represent YCl₂- and YBr₂-layer characters.

total magnetic moment is $0.00 \mu_B$, thus becoming a fully-compensated ferrimagnet even if $U=0.00$ eV. When CrI₃/CrGeTe₃ heterojunction is in the FM state, it remains a semiconductor with a total magnetic moment of $12 \mu_B$, which is precisely the sum of the total magnetic moments of the two independent monolayers. As we proposed earlier, even stacking two different antiferromagnets can also achieve fully-compensated ferrimagnetism. When a/a_0 is less than 0.968, CrI₃/CrGeTe₃ heterojunction is in such a situation, characterized by a zero-net total magnetic moment and weak spin-splitting (The expanded conduction band near the Fermi level is shown in FIG.S3.[39]). This example further illustrates that stacking two different AFM monolayers to achieve fully-compensated ferrimagnetism is not conducive to a large spin-splitting.

We have also considered other heterostructures to illustrate the universality of our proposal. The YBr₂ and YCl₂ monolayers have been predicted to be stable FM semiconductors with GGA+ U ($U=2.00$ eV)[41]. The AB-stacked YBr₂/YCl₂ heterojunction (see Figure 5 (a)) is constructed with an AFM1 magnetic ground state. The total magnetic moment of YBr₂/YCl₂ heterojunction is $0.00 \mu_B$, which is further confirmed by the fact that the IDOSs of the two spin channels are the same within the band gap (see Figure 5 (b)). According to Figure 5 (c) and (d), the calculated band structures show that YBr₂/YCl₂ heterojunction possesses a pronounced

spin-splitting and a type-II heterojunction (The type of the heterojunction depends on the magnitude of U). Therefore, YBr₂/YCl₂ heterojunction can achieve fully-compensated ferrimagnetism.

We have also constructed AB-stacked CrI₃/CrBr₃ heterostructure (see FIG.S4[39]) using experimentally synthesized CrI₃ and CrBr₃ monolayers[30, 42]. Unfortunately, within a reasonable range of U , the CrI₃/CrBr₃ heterostructure always maintains a FM ground state. Nevertheless, we have also calculated its electronic structure with the AFM1 magnetic ordering. Its total magnetic moment is indeed $0.00 \mu_B$, and there is a pronounced spin-splitting (see FIG.S4[39]). A large number of 2D FM monolayers have been theoretically predicted[43], thus enabling the creation of a multitude of heterojunctions with zero-net-magnetization. The most crucial aspect here is that, to achieve fully-compensated ferrimagnetism, these heterojunctions should possess A-type AFM ordering, which can be simply estimated through an electron-counting rule[44].

Discussion and conclusion.— The interface of vertical heterostructures is maintained by weak vdW forces, which do not require strict lattice matching and allow the combination of materials with different lattice constants. This is more conducive to realizing our proposal in a wider range of 2D FM materials. Achieving altermagnetism through the stacking of bilayer has symmetry requirements[5, 45, 46], that is to say, it is very sensitive to the stacking manner, which poses a challenge for experimental realization. Our proposal to achieve fully-compensated ferrimagnetism does not have any symmetry requirements for the stacking manner. As long as the A-type AFM coupling is satisfied, a fully-compensated ferrimagnet with pronounced spin-splitting can be achieved. These advantages are highly conducive to the experimental realization of fully-compensated ferrimagnetism.

In summary, the vertical heterostructures are proposed with two different but equally magnetized 2D ferromagnetic materials to achieve a fully-compensated ferrimagnet. This approach is insensitive to lattice matching and stacking manner, facilitating experimental realization. First-principles calculations show that CrI₃/CrGeTe₃ heterojunction can form a fully-compensated ferrimagnet with pronounced spin-splitting, and tensile strain can enhance this state. Our work provides a feasible strategy for experimentally realizing fully-compensated ferrimagnetism.

This work is supported by Natural Science Basis Research Plan in Shaanxi Province of China (2025JC-YBMS-008). Y.S.A. is supported by the Singapore Ministry of Education Academic Research Fund Tier 2 (Award No. MOE-T2EP50221-0019). We are grateful to Shanxi Supercomputing Center of China, and the calculations were performed on TianHe-2.

* sandongyuwang@163.com

† These authors contributed equally to this work.

- [1] X. Hu, Half-metallic antiferromagnet as a prospective material for spintronics, *Adv. Mater.* **24**, 294 (2012).
- [2] T. Jungwirth, J. Sinova, A. Manchon, X. Marti, J. Wunderlich and C. Felser, The multiple directions of antiferromagnetic spintronics, *Nat. Phys.* **14**, 200 (2018).
- [3] L. Šmejkal, J. Sinova and T. Jungwirth, Beyond conventional ferromagnetism and antiferromagnetism: A phase with nonrelativistic spin and crystal rotation symmetry, *Phys. Rev. X* **12**, 031042 (2022).
- [4] I. Mazin, Altermagnetism—a new punch line of fundamental magnetism, *Phys. Rev. X* **12**, 040002 (2022).
- [5] Y. Liu, J. Yu and C. C. Liu, Twisted Magnetic Van der Waals Bilayers: An Ideal Platform for Altermagnetism, *Phys. Rev. Lett.* **133**, 206702 (2024).
- [6] X. Duan, J. Zhang, Z. Zhang, I. Žutić and T. Zhou, Antiferroelectric Altermagnets: Antiferroelectricity Alters Magnets, *Phys. Rev. Lett.* **134**, 106801 (2025).
- [7] H.-Y. Ma, M. L. Hu, N. N. Li, J. P. Liu, W. Yao, J. F. Jia and J. W. Liu, Multifunctional antiferromagnetic materials with giant piezomagnetism and noncollinear spin current, *Nat. Commun.* **12**, 2846 (2021).
- [8] M. Gu, Y. Liu, H. Zhu, K. Yananose, X. Chen, Y. Hu, A. Stroppa and Q. Liu, Ferroelectric Switchable Altermagnetism, *Phys. Rev. Lett.* **134**, 106802 (2025).
- [9] S. D. Guo, Hidden altermagnetism, *Front. Phys. (Beijing)* **21**, 025201 (2026).
- [10] L. Bai, W. Feng, S. Liu, L. Šmejkal, Y. Mokrousov, and Y. Yao, Altermagnetism: Exploring New Frontiers in Magnetism and Spintronics, *Adv. Funct. Mater.* **34**, 2409327 (2024).
- [11] S. D. Guo, X. S. Guo, D. C. Liang and G. Wang, Symmetry-breaking induced transition among net-zero-magnetization magnets, *J. Mater. Chem. C* **13**, 11997 (2025).
- [12] H. van Leuken and R. A. de Groot, Half-Metallic Antiferromagnets, *Phys. Rev. Lett.* **74**, 1171 (1995).
- [13] H. Akai and M. Ogura, Half-Metallic Diluted Antiferromagnetic Semiconductors, *Phys. Rev. Lett.* **97**, 026401 (2006).
- [14] S. Wurmehl, H. C. Kandpal, G. H. Fecher, and C. Felser, Valence electron rules for prediction of half-metallic compensated-ferrimagnetic behaviour of Heusler compounds with complete spin polarization, *J. Phys.: Condens. Matter* **18**, 6171 (2006).
- [15] T. Kawamura, Kazuyoshi Yoshimi, Kenichiro Hashimoto, Akito Kobayashi and Takahiro Misawa, Compensated Ferrimagnets with Colossal Spin Splitting in Organic Compounds, *Phys. Rev. Lett.* **132**, 156502 (2024).
- [16] M. Žic, K. Rode, N. Thiagarajah, Y. C. Lau, D. Betto, J. M. D. Coey, S. Sanvito, K. J. O'Shea and C. A. Ferguson, Designing a fully compensated half-metallic ferrimagnet, *Phys. Rev. B* **93**, 140202(R) (2016).
- [17] H. A. Zhou, T. Xu, H. Bai and W. Jiang, Efficient Spintronics with Fully Compensated Ferrimagnets, *J. Phys. Soc. Jpn.* **90**, 081006 (2021).
- [18] I. Galanakis and E. Sasoğlu, High T_C half-metallic fully-compensated ferrimagnetic Heusler compounds, *Appl. Phys. Lett.* **99**, 052509 (2011).
- [19] X. Y. Hou, Z. F. Gao, H. C. Yang, P. J. Guo and Z. Y. Lu, Luttinger compensated magnetic material $\text{LaMn}_2\text{SbO}_6$, *arXiv:2504.09447* (2025).
- [20] Y. Liu, S. D. Guo, Y. Li and C. C. Liu, Two-dimensional fully-compensated Ferrimagnetism, *Phys. Rev. Lett.* **134**, 116703 (2025).
- [21] S. D. Guo, Valley polarization in two-dimensional zero-net-magnetization magnets, *Appl. Phys. Lett.* **126**, 080502 (2025).
- [22] S. D. Guo, Y. L. Tao, Z. Y. Zhuo, G. Zhu and Y. S. Ang, Electric-field-tuned anomalous valley Hall effect in A-type hexagonal antiferromagnetic monolayers, *Phys. Rev. B* **109**, 134402 (2024).
- [23] S. D. Guo, W. Xu, Y. Xue, G. Zhu and Y. S. Ang, Layer-locked anomalous valley Hall effect in a two-dimensional A-type tetragonal antiferromagnetic insulator, *Phys. Rev. B* **109**, 134426 (2024).
- [24] S. D. Guo, P. Li and G. Wang, First-principles calculations study of valley polarization in antiferromagnetic bilayer systems, *Phys. Rev. B* **111**, L140404 (2025).
- [25] L. Zhang, S. D. Guo and G. Wang, Spontaneous and reversible spin-splitting in ferroelectric A-type antiferromagnetism, *J. Mater. Chem. C* **12**, 8485 (2024).
- [26] J. Feng, X. Zhou, J. Chen, M. Xu, X. Yang and Y. Li, Ferroelectric antiferromagnetic lifting of spin-valley degeneracy, *Phys. Rev. B* **111**, 214446 (2025).
- [27] N. Cheng, H. Cheng, X. Zhao, G. Hu, X. Yuan and J. Ren, Ferroelectric polarization manipulates the layer-polarized anomalous Hall effect in bilayers with fully compensated ferrimagnetism, *Phys. Rev. B* **111**, 195154 (2025).
- [28] F. Yao, M. Liao, M. Gibertini et al., Switching on and off the spin polarization of the conduction band in antiferromagnetic bilayer transistors, *Nat. Nanotechnol.* **20**, 609 (2025).
- [29] S. D. Guo, S. Chen and G. Wang, Spin ordering-induced fully-compensated ferrimagnetism, *arXiv:2507.10848* (2025).
- [30] B. Huang, G. Clark, E. Navarro-Moratalla et al., Layer-dependent ferromagnetism in a van der Waals crystal down to the monolayer limit, *Nature* **546**, 270 (2017).
- [31] C. Gong, L. Li, Z. Li et al., Discovery of intrinsic ferromagnetism in two-dimensional Van der Waals crystals, *Nature* **546**, 265 (2017).
- [32] P. Hohenberg and W. Kohn, Inhomogeneous Electron Gas, *Phys. Rev.* **136**, B864 (1964); W. Kohn and L. J. Sham, Self-Consistent Equations Including Exchange and Correlation Effects, *Phys. Rev.* **140**, A1133 (1965).
- [33] G. Kresse, Ab initio molecular dynamics for liquid metals, *J. Non-Cryst. Solids* **193**, 222 (1995).
- [34] G. Kresse and J. Furthmüller, Efficiency of ab-initio total energy calculations for metals and semiconductors using a plane-wave basis set, *Comput. Mater. Sci.* **6**, 15 (1996).
- [35] G. Kresse and D. Joubert, From ultrasoft pseudopotentials to the projector augmented-wave method, *Phys. Rev. B* **59**, 1758 (1999).
- [36] J. P. Perdew, K. Burke and M. Ernzerhof, Generalized gradient approximation made simple, *Phys. Rev. Lett.* **77**, 3865 (1996).
- [37] S. L. Dudarev, G. A. Botton, S. Y. Savrasov, C. J. Humphreys, and A. P. Sutton, Electron-energy-loss spectra and the structural stability of nickel oxide: An LSDA+U study, *Phys. Rev. B* **57**, 1505 (1998).
- [38] S. Grimme, S. Ehrlich and L. Goerigk, Effect of the

- damping function in dispersion corrected density functional theory, *J. Comput. Chem.* **32**, 1456 (2011).
- [39] See Supplemental Material at [] for the crystal structures, the integrated densities of states and the related energy band structures.
- [40] S. D. Guo, W. Q. Mu and B. G. Liu, Valley-polarized quantum anomalous Hall insulator in monolayer, *2D Mater.* **9**, 035011 (2022).
- [41] B. Huang, W.-Y. Liu, X.-C. Wu, S.-Z. Li, H. Li, Z. Yang and W.-B. Zhang, Large spontaneous valley polarization and high magnetic transition temperature in stable two-dimensional ferrovalley YX_2 ($X=I, Br, \text{ and } Cl$), *Phys. Rev. B* **107**, 045423 (2023).
- [42] W. Chen, Z. Sun, Z. Wang, L. Gu, X. Xu, S. Wu and C. Gao, Direct observation of van der Waals stackingdependent interlayer magnetism, *Science* **366**, 983 (2019).
- [43] S. Xing, J. Zhou, X. Zhang, S. Elliott and Z. Sun, Theory, properties and engineering of 2D magnetic materials, *Rog. Mater. Sci.* **132**, 101036 (2023).
- [44] J. Xiao and B. Yan, An electron-counting rule to determine the interlayer magnetic coupling of the van der Waals materials, *2D Mater.* **7**, 045010 (2020).
- [45] S. Zeng and Y.-J. Zhao, Bilayer stacking -type altermagnet: A general approach to generating two-dimensional altermagnetism, *Phys. Rev. B* **110**, 174410 (2024).
- [46] W. Sun, H. Ye, L. Liang, N. Ding, S. Dong and S.-S. Wang, Stacking-dependent ferroicity of a reversed bilayer: Altermagnetism or ferroelectricity. *Phys. Rev. B* **110**, 224418 (2024).